Transmission and Anderson localization in dispersive metamaterials

Ara A. Asatryan,[1] Lindsay C. Botten,[1] Michael A. Byrne,[1] Valentin D. Freilikher,[2] Sergey A. Gredeskul,[3,4]
Ilya V. Shadrivov,[4] Ross C. McPhedran,[5] and Yuri S. Kivshar[4]

[1]*Department of Mathematical Sciences and Centre for Ultrahigh-bandwidth Devices for Optical Systems (CUDOS),
University of Technology, Sydney, NSW 2007, Australia*
[2]*Department of Physics, Bar-Ilan University, Raman-Gan 52900, Israel*
[3]*Department of Physics, Ben Gurion University of the Negev, Beer Sheva 84105, Israel*
[4]*Nonlinear Physics Center and CUDOS, Australian National University, Canberra, ACT 0200, Australia*
[5]*School of Physics and CUDOS, University of Sydney, Sydney, NSW 2006, Australia*
(Received 2 September 2011; revised manuscript received 26 November 2011; published 23 January 2012)

Comprehensive theoretical and numerical studies of the effects of dispersion and absorption on the Anderson localization of classical waves in weakly disordered, one-dimensional stacks composed of dispersive metamaterials and normal materials are presented. An asymptotic analysis for studying the effects of dispersion and absorption is developed. It is shown that the localization of waves in random stacks composed entirely of either metamaterial or normal dielectric layers is completely suppressed at frequencies where the magnetic permeability or the dielectric permittivity is zero. In mixed stacks of alternating layers of normal and metamaterials with disorder present in either the dielectric permittivity or the magnetic permeability, localization is substantially suppressed not only at these frequencies but in essentially wider frequency ranges. When both the permittivity and the permeability are random, the localization behavior is similar to that in monotype stacks. At the transition from a double negative metamaterial to a single negative metamaterial, the transmission length drops dramatically in a manner that might be useful in optical switching. Polarization effects are also considered and it is shown that localization is suppressed at the Brewster angle, in a manner dependent on both the polarization and the nature of the disorder. Theoretical predictions are in excellent agreement with numerical calculations.

PACS number(s): 42.25.Dd, 42.25.Fx

I. INTRODUCTION

Anderson localization[1] is one of the most fundamental concepts in physics.[2] Localization of light in random media has been investigated intensively during the last few decades, with one-dimensional (1D) strong localization receiving the most comprehensive study. Recently, the emergence of metamaterials—a new class of artificial materials with negative refractive index—has sparked considerable interest from researchers and engineers; see, for example, Refs. 3–7. Metamaterials are also referred to as double-negative materials (DNMs), associated with permittivity and permeability whose real parts are both negative, in contrast with single-negative materials (SNMs), in which either the real part of the dielectric permeability or the real part of the magnetic permittivity is negative.

Since, today, all available metamaterials are manmade, they usually contain technological imperfections or faults. The first consideration of manufacturing defects in magnetic metamaterials showed that imperfections could have a strong impact on propagation.[8] Further studies showed that Anderson localization in metamaterials is suppressed, either partially or completely, compared to localization in conventional materials. A rich vein of new phenomena related to such suppression has been revealed recently. In one-dimensional stacks comprising alternating layers of normal and metamaterials, with only thickness disorder, delocalization can occur at a single frequency at which the impedances of layers match.[9] Disorder in the dielectric permittivity of the layers (in the absence of thickness disorder) also gives rise to a startling suppression of localization at long wavelengths.[10] This suppression is so

strong that there is a change in the functional dependence $l \sim \lambda^\kappa$ of the localization length at long wavelengths. From the well-known, classical value of $\kappa = 2$, this exponent increases to a much larger value, estimated in Ref. 10 as $\kappa \approx 6$, i.e., the λ^6 anomaly. In mixed stacks with weak, long correlated disorder of the layer thicknesses, the frequency regions corresponding to complete delocalization (pass bands) are essentially wider than those for conventional right-handed stacks.[11] Complete delocalization occurs at special frequencies and special angles of incidence corresponding to the Brewster anomaly.[12]

While further studies[12–14] confirmed the λ^6 anomaly, more detailed numerical calculations for very long stacks[15] showed that the exponent κ may increase to larger values, up to $\kappa \approx 8.78$, for a stack of approximately 10^{12} layers. As is reported in Ref. 12, off-axis incidence, by a a small angle, can affect this functional dependence. However, the introduction of correlation in the disorder has little effect.[14] The consideration of layers with different thicknesses,[16] or the introduction of the layer thickness disorder, in addition to the material parameters disorder, strongly enhances localization.[15,17] In Ref. 17 it is shown that because of specific, nonuniform phase distribution, in the second order of disorder, localization is completely destroyed for long waves, and that fourth-order calculations are required. Eventually, in a recent paper,[18] the long-wave dependence of $l \sim \lambda^8$ was analytically established, showing that the anomaly which was discovered numerically in Refs. 10 and 15 was actually a λ^8 anomaly.

Localization in SNMs has also been considered,[19] with it being shown that the localization length can be smaller than the decay length of the corresponding periodic structure. The suppression of localization has been reported also in

one-dimensional metamaterial superlattices with thickness disorder.[12]

All metamaterials inherently exhibit dispersion and absorption, and this has to be taken into account in any realistic study of localization. While the dispersive effects on localization in normal materials have been considered in Ref. [20], the corresponding study for metamaterials has only started.[13,14] The first of these papers is devoted to light propagation through one-dimensional photonic disordered quasiperiodic superlattices, composed of alternating layers with random thicknesses of air and a dispersive metamaterial. In the second one, the effects of disorder correlations on light propagation and Anderson localization in one-dimensional dispersive metamaterials are studied.

Of particular interest are dispersive materials, in which real parts of the dielectric permittivity or magnetic permeability may vanish at some frequencies. Structures containing metamaterials with $\varepsilon \approx 0$ have been studied most intensively.[21–23] It has been shown in particular that energy may propagate through ultranarrow waveguide channels in such structures.[24,25] It is thus interesting and important to investigate localization in samples with ε-near-zero (ENZ), i.e., with $\varepsilon \approx 0$, and in μ-near-zero (MNZ) materials, with $\mu \approx 0$.

In this paper, we examine transport and localization in one-dimensional disordered systems with different types of dispersive metamaterials, and predict a new instance of delocalization. We prove theoretically, and through numerical simulations, that, in systems with $\varepsilon = 0$ or $\mu = 0$, the field is delocalized in the presence of either dielectric permittivity disorder, magnetic permeability disorder, or thickness disorder. This is in contrast to delocalization at the Brewster angle that occurs in the presence of solely thickness disorder.

In Sec. II, we describe the theoretical model and present the asymptotic analysis based on the extension of the approach developed in Ref. [15]. The analysis of delocalization in ENZ or MNZ disordered stacks and the study of polarization effects are presented in Secs. II C 1 and II C 2, respectively. Numerical simulations and comparisons with the asymptotic predictions are presented in Sec. III, comprising the characterization of localization in monotype stacks (Secs. III A and III B) and in mixed alternating stacks (Sec. III C).

II. THEORETICAL CONSIDERATION

A. Description of the model

We consider a one-dimensional stack which consists of an even number N of layers. The stack may be either monotype, in which case each layer is either a metamaterial (A) layer or a normal material (B) layer, or mixed, comprising alternating A and B layers, as shown in Fig. 1. All layers have the same thickness $d = 0.003$ m, which is consistent with manufactured metamaterials.[26]

The dielectric permittivity and the magnetic permeability of the metamaterial layers as functions of a circular frequency f are described by the Lorentz oscillator model

$$\varepsilon(f) = 1 - \frac{f_{ep}^2 - f_e^2}{f^2 - f_e^2 + i\gamma f}, \tag{1}$$
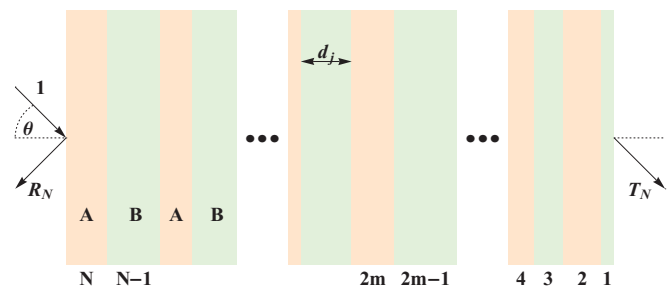

FIG. 1. (Color online) The geometry of the model. θ denotes the angle of incidence from free space.

$$\mu(f) = 1 - \frac{f_{mp}^2 - f_m^2}{f^2 - f_m^2 + i\gamma f}. \tag{2}$$

Here f_m and f_e are the resonance frequencies and γ is the absorption parameter. In our model, disorder enters the problem through random resonance frequencies so that

$$f_e = \bar{f}_e(1 + \delta_e), \quad f_m = \bar{f}_m(1 + \delta_m), \tag{3}$$

where $\bar{f}_{e,m} = \langle f_{e,m} \rangle$ are the mean resonance frequencies (with the angle brackets denoting ensemble averaging) and $\delta_{e,m}$ are independent random values distributed uniformly in the ranges $[-Q_{e,m}, Q_{e,m}]$. The characteristic frequencies f_{mp} and f_{ep} are nonrandom. Therefore, in lossless media ($\gamma = 0$), both the magnetic permeability and the dielectric permittivity vanish with their mean values, $\bar{\varepsilon}(f) = \langle \varepsilon(f) \rangle$ and $\bar{\mu}(f) = \langle \mu(f) \rangle$, at frequencies $f = f_{ep}$ and $f = f_{mp}$, respectively; i.e.,

$$\mu(f_{mp}) = \bar{\mu}(f_{mp}) = 0, \quad \varepsilon(f_{ep}) = \bar{\varepsilon}(f_{ep}) = 0. \tag{4}$$

Following Refs. [26] and [27], in our numerical calculations we choose the values of characteristic frequencies $f_{mp} = 10.95$ GHz, $f_{m0} = \bar{f}_m = 10.05$ GHz, $f_{ep} = 12.8$ GHz, $f_{e0} = \bar{f}_e = 10.3$ GHz, and $\gamma = 10$ MHz, which fit the experimental data given in Ref. [26]. That is, we are using a model based on experimentally measured values for the metamaterial parameters. Then we choose the maximal widths of the distributions of the random parameters $\delta_{e,m}$ as $Q_{e,m} \leqslant 5 \times 10^{-3}$, corresponding to weak disorder.

We focus our study on the frequency region 10.40 GHz $< f <$ 11.00 GHz. In the absence of absorption and disorder, for these frequencies the dielectric permittivity and the magnetic permeability of the metamaterial layers vary over the intervals $-26.9 < \varepsilon < -2.9$ and $-1.64 < \mu < 0.055$. The refractive index is negative in the frequency range 10.40 GHz $< f < f_{mp} = 10.95$ GHz, as shown in the inset of Fig. 2. However, at $f_{mp} = 10.95$ GHz, the magnetic permeability changes sign and the metamaterial changes from being double negative (DNM) to single negative (SNM). As we show later, such changes have a profound effect on the localization properties.

In generic normal dielectric layers with a similar dispersion, the values of the dielectric permittivity and the magnetic permeability are set to be $-\varepsilon^*(f)$ and $-\mu^*(f)$, respectively, where $\varepsilon(f)$ and $\mu(f)$ are given by Eqs. (1) and (2) and the asterisk ($*$) denotes complex conjugation. In the region 10.40 GHz $< f <$ 10.95 GHz, the refractive index is positive and at higher frequencies 10.95 GHz $< f <$ 11.00 GHz the

magnetic permittivity becomes negative and so the material becomes a SNM.

In Sec. III B 2, we consider a specific model for which the dielectric permittivity coincides with that of normal material, $-\varepsilon^*(f)$, in the range of frequencies 10.40 GHz $< f <$ 11.00 GHz, while the magnetic permeability coincides with $-\mu^*(f)$ only in the region 10.40 GHz $< f <$ 10.95 GHz, and at higher frequencies, 10.95 GHz $< f <$ 11.00 GHz, is equal to $\mu(f)$. As a consequence of this exotic choice, the refractive index is positive in the entirety of the studied frequency region, aside from $f = 10.95$ GHz at which it vanishes.

B. Analytical treatment

In what follows, we study the transmission of a plane wave incident on a random stack from free space, as shown in Fig. 1. The plane wave may be either *s* or *p* polarized where we adopt the conventional definition for polarization, in which *s* and *p* polarizations refer respectively to the cases where the electric and magnetic fields are perpendicular to the plane of incidence. Due to Anderson localization, the transmission coefficient T_N of a plane wave propagating through a sufficiently long stack exponentially decays with its length Nd. This decay is described by the transmission length l_T, measured in units of the mean thickness d of each layer (for details see Ref. 15), and which we define as

$$l_T(N) = -\frac{N}{\langle \ln |T_N| \rangle}. \tag{5}$$

In the limit $N \to \infty$, the transmission length l_T coincides with the localization length l:

$$l = \lim_{N \to \infty} l_T.$$

Accordingly, in numerical simulations for calculating the localization length, it is necessary to generate random realizations that are sufficiently long for the condition $N \gg l_T$ to hold.

In Refs. 10, 15 and 28 an effective method for studying the transport and localization in random stacks composed of the weakly reflecting layers has been developed. In the dispersive case considered in the present paper, the reflection from a layer located in free space is not necessarily weak, in which instance the method is inapplicable.

However, as localization properties of a random stack are intrinsic properties of the stack, they cannot, and must not, depend on the material properties of the exterior medium, i.e., free space in this case. Accordingly, the localization length can be calculated from

$$l = -\lim_{N \to \infty} \frac{2N}{\ln |T_N|^2} = -\lim_{N \to \infty} \frac{2N}{\ln |\hat{T}_N|^2}, \tag{6}$$

where $\hat{T}_N$ is the transmission coefficient of a stack embedded in an exterior medium with permittivity and permeability given by the mean values of $\bar{\varepsilon}$ and $\bar{\mu}$, respectively. The connection to the outside medium through the "leads" (a circuit theory term borrowed to describe thin coupling layers) can only change the coupling conditions to the random stack through the angle of incidence. The proof of this statement is given in the Appendix to this paper.

Therefore, instead of vacuum, we consider that the layers are embedded in an effective medium with the dielectric permittivity $\bar{\varepsilon}(f) \equiv \langle \varepsilon(f) \rangle$ and magnetic permeability $\bar{\mu}(f) \equiv \langle \mu(f) \rangle$. In such circumstances, the reflection coefficient is always small and we may apply the method derived in Refs. 10, 15 and 28. It is important to note that while in the localized regime the input and output media are of no significance, they do play a crucial role when localization breaks down (see the following Sec. II C).

Following Refs. 10 and 15 we employ the exact recurrence relations for the total transmission (T_n) and reflection (R_n) coefficients

$$T_n = \frac{T_{n-1} t_n}{1 - R_{n-1} r_n}, \tag{7}$$

$$R_n = r_n + \frac{R_{n-1} t_n^2}{1 - R_{n-1} r_n}, \quad n \geqslant 2, \tag{8}$$

with the initial conditions $T_0 = 1$ and $R_0 = 0$. Here r_n and t_n are the reflection and the transmission coefficients of the single nth layer embedded in the effective medium with mean dielectric permittivity $\bar{\varepsilon}(f) \equiv \langle \varepsilon(f) \rangle$ and magnetic permeability $\bar{\mu}(f) \equiv \langle \mu(f) \rangle$. That is,

$$r_n = \frac{\rho_n (1 - e^{2i\beta_n})}{1 - \rho_n^2 e^{2i\beta_n}}, \tag{9}$$

$$t_n = \frac{(1 - \rho_n^2) e^{i\beta_n}}{1 - \rho_n^2 e^{2i\beta_n}}. \tag{10}$$

In Eqs. (9) and (10), $\beta_n = k d v_n \cos \theta_n$, $v_n = \sqrt{\varepsilon_n \mu_n}$, k is the free-space wave number $k = 2\pi / \lambda_0$, and the interface Fresnel reflection coefficient ρ_n is given by

$$\rho_n = \frac{Z_b \cos \theta_b - Z_n \cos \theta_n}{Z_b \cos \theta_b + Z_n \cos \theta_n}. \tag{11}$$

The impedances Z_b and Z_n are

$$Z_b = \begin{cases} \sqrt{\bar{\mu}/\bar{\varepsilon}} & p \text{ polarization}, \\ \sqrt{\bar{\varepsilon}/\bar{\mu}} & s \text{ polarization}, \end{cases} \tag{12}$$

$$Z_n = \begin{cases} \sqrt{\mu_n/\varepsilon_n} & p \text{ polarization}, \\ \sqrt{\varepsilon_n/\mu_n} & s \text{ polarization}. \end{cases} \tag{13}$$

The angles θ_b and θ_n satisfy Snell's law

$$v_n \sin \theta_n = \bar{v} \sin \theta_b = \sin \theta_a, \quad \bar{v} = \sqrt{\bar{\varepsilon}\bar{\mu}}, \tag{14}$$

$$\sin \theta_b = \frac{\sin \theta_a}{\sqrt{\bar{\varepsilon}(f)}\sqrt{\bar{\mu}(f)}}, \tag{15}$$

where θ_a is the external angle of incidence from free space. These expressions are equally applicable for both normal and metamaterial slabs[29] with the corresponding choice of the square root branch. Note, however, that for a fixed angle of incidence θ_a [from free space (air)], it follows that the angle θ_b will vary with frequency, due to dispersion (15).

In the limit of weak disorder ($|r_n| \ll 1$), Eqs. (7) and (8) can be linearized and written as

$$\ln T_n = \ln T_{n-1} + \ln t_n + R_{n-1} r_n, \tag{16}$$

$$R_n = r_n + R_{n-1} t_n^2, \quad n \geqslant 2. \tag{17}$$

For this case, the localization length has been calculated in Ref. 15 for monotype-stack (composed of either

double-negative metamaterial layers or normal material layers) samples

$$\frac{1}{l} = -\text{Re}\,\langle \ln t_n \rangle - \text{Re}\,\frac{\langle r_n \rangle^2}{1 - \langle t_n^2 \rangle}, \qquad (18)$$

and for mixed stacks of alternating normal and metamaterial layers,

$$\frac{1}{l} = -\text{Re}\,\langle \ln t_n \rangle - \frac{|\langle r_n \rangle^2| + \text{Re}\,\left(\langle r_n \rangle^2 \langle t_n^2 \rangle^*\right)}{1 - |\langle t_n^2 \rangle|^2}. \qquad (19)$$

C. Suppression of localization in disordered stacks

Dispersion affects dramatically the transport properties of the disordered medium. In particular, the localization can be suppressed either at some angle of incidence or at a selected frequency, or even in a finite frequency range. The first two cases are studied below (Secs. II C 1 and II C 2), while the third one is considered in Sec. III C.

1. Power decay of the transmission coefficient at normal incidence in the vicinity of μ- or ε- near-zero points

The localization length in *a lossless, nondispersive, monotype meta- or normal-material random stack* increases in the long-wave region as $\sim\lambda^2$; see Ref. 15. In the presence of dispersion, the first term in Eq. (18) is dominant, and the long-wave asymptotic of the localization length manifests the same behavior according to

$$\frac{1}{l} = \frac{\pi^2 d^2}{2\lambda^2(f)}\left(\frac{\langle \mu^2 \rangle}{\langle \mu \rangle^2} + \frac{\langle \varepsilon^2 \rangle}{\langle \varepsilon \rangle^2} - 2\right), \qquad (20)$$

in which we have omitted the subscript n.

The distinctive property of dispersive media is that the wavelength $\lambda(f)$ in the medium given by

$$\lambda(f) = \frac{\lambda_0(f)}{\sqrt{\varepsilon(f)\mu(f)}} \qquad (21)$$

is frequency dependent, and can be large even when the wavelength of the incident signal, $\lambda_0(f) = 2\pi/k = c/f$, is small.

Accordingly, the inverse localization length

$$l^{-1} \propto f^2 \varepsilon(f)\mu(f) \qquad (22)$$

becomes small not only at low frequencies $f \to 0$ but also in the vicinity of μ- or ε-zero points. For example, as the frequency approaches the μ-zero point from below, i.e., $f \to f_{mp}^-$, in *a monotype stack of random metamaterial layers*, $\mu(f)$, for any realization, is proportional to the difference $(f_{mp} - f)$ and the expression for localization length diverges as $(f_{mp} - f)^{-1}$. Formally, this divergence can be treated as delocalization; however, the limiting value $1/l = 0$ means nothing but the absence of exponential localization. Moreover, when the localization length becomes larger than the size of the stack, ballistic transport occurs and the transmission coefficient is determined by transmission length, (5), rather than by the localization length.

To calculate the transmission coefficient for this case we consider, for the sake of simplicity, *a stack with only ε disorder.*

Here the transfer matrix of the nth layer at $f = f_{mp}$ has the form

$$\mathcal{T}_n \equiv \mathcal{T}(\epsilon_n) = \begin{pmatrix} 1 + \epsilon_n & \epsilon_n \\ -\epsilon_n & 1 - \epsilon_n \end{pmatrix}, \quad \epsilon_n = \frac{ikd\varepsilon_n}{2}.$$

As a consequence of the easily verified property

$$\mathcal{T}(\epsilon_1)\mathcal{T}(\epsilon_2) = \mathcal{T}(\epsilon_1 + \epsilon_2), \qquad (23)$$

it follows that the stack transfer matrix $\mathcal{T}$ is

$$\mathcal{T} = \prod_{n=1}^{N} \mathcal{T}(\epsilon_n) = \begin{bmatrix} 1 + \mathcal{E} & \mathcal{E} \\ -\mathcal{E} & 1 - \mathcal{E} \end{bmatrix},$$

where

$$\mathcal{E} = \frac{ikL}{2}\frac{1}{N}\sum_{n=1}^{N}\varepsilon_n, \quad L = Nd. \qquad (24)$$

In a sufficiently long stack, $\mathcal{E} \approx \frac{1}{2}ikL\bar{\varepsilon}$ and the transmittance $T = |\mathcal{T}_{11}|^{-2}$ is given by

$$T = \frac{1}{1 + \left(\frac{kL\bar{\varepsilon}(f)}{2}\right)^2}. \qquad (25)$$

Thus, at the frequency f_{mp}, the transmittance of the sample is not an exponentially decreasing function of the length L (as is typical for 1D Anderson localization). It decreases much more slowly, namely, according to the power law $T \propto L^{-2}$.

There are two physical explanations for the delocalization described above. First, at a μ-zero point ($f = f_{mp}$), the refractive index ν_n vanishes together with the phase terms $\beta_n = kd\nu_n \cos\theta_n$ across the layer, thereby weakening the interference, which is the main cause of localization. Second, the effective wavelength inside the stack tends to infinity when $\mu \to 0$ and exceeds the stack length. Obviously, such a wave is insensitive to disorder and therefore cannot be localized.

In the limit as the frequency approaches the μ-zero frequency, from above, i.e., $f \to f_{mp}^+$, the medium is single negative and $\varepsilon\mu < 0$. For frequencies f not too close to f_{mp}, the radiation decays exponentially inside the sample due to tunneling, and in the absence of dissipation the decay rate is

$$l = \frac{1}{kd\sqrt{-\langle \mu \rangle \langle \varepsilon \rangle}}. \qquad (26)$$

Thus, as we approach the μ-zero frequency from the right, the formally calculated localization length diverges as $l \propto (f - f_{mp})^{-1/2}$, i.e., much more slowly than for the left-hand limit for which $l \propto (f_{mp} - f)^{-1}$. The transport properties in the vicinity of the ε-zero frequency f_{ep} can be considered in a similar manner. Waves are also delocalized in the more exotic case when both dielectric permittivity and magnetic permeability vanish simultaneously. The vanishing of both μ and ε simultaneously can happen at Dirac points in photonic crystals.[30]

The use of off-axis incidence from free space for frequencies for which μ or ε are zero is not an appropriate mechanism for probing the suppression of localization. In such circumstances, tunneling occurs and the localization properties of the stack are not "accessible" from free space. Nevertheless, suppression of localization can be revealed using an internal probe, e.g., by placing a plane-wave source inside the

stack, or by studying the corresponding Lyapunov exponent. Both approaches show total suppression of localization at the frequencies at which dielectric permittivity or magnetic permeability vanish.

In such circumstances, each layer which is embedded in a homogeneous medium with material constants given by the average values of the dielectric permittivity and magnetic permeability is completely transparent, with this manifesting the complete suppression of localization. However the "delocalized" states at the zero-μ or zero-ε frequencies are in a sense trivial, corresponding to fields which do not change along the direction normal to the layers.

2. Brewster anomaly

We now consider another example of the suppression of localization, this time related to the Brewster anomaly. It has been shown in Ref. 28 that in a *one-dimensional nondispersive mixed stack with only thickness disorder*, delocalization of *p*-polarized radiation occurs at the Brewster angle of incidence. At this angle, the Fresnel coefficient ρ [Eq. (11)] and, therefore, the reflection coefficient [Eq. (9)] as well, vanish for any frequency, thus making each layer completely transparent.

In the presence of dispersion, the same condition $\rho = 0$ leads to more intriguing results. In this instance, frequency-dependent angles, at which a layer with the dielectric permittivity $\varepsilon(f)$ and magnetic permeability $\mu(f)$ embedded in the effective medium with mean dielectric permittivity $\overline{\varepsilon}(f)$ and magnetic permeability $\overline{\mu}(f)$ becomes transparent, exist not only for *p* polarization but also for an *s*-polarized wave. This means that the Brewster anomaly occurs for both polarizations, with the corresponding angles, θ_p and θ_s, being determined by the conditions

$$\tan^2 \theta_p = \frac{\varepsilon(\varepsilon\overline{\mu} - \overline{\varepsilon}\mu)}{\overline{\varepsilon}(\varepsilon\mu - \overline{\varepsilon}\,\overline{\mu})}, \tag{27}$$

$$\tan^2 \theta_s = \frac{\mu(\overline{\varepsilon}\mu - \varepsilon\overline{\mu})}{\overline{\mu}(\varepsilon\mu - \overline{\mu}\,\overline{\varepsilon})}. \tag{28}$$

It can be shown that the right-hand sides of these equations (the Brewster conditions) always have opposite signs. From Eqs. (27) and (28) one can find either the Brewster angle for a given frequency or the Brewster frequency for a given angle of incidence.

While for a stack with only thickness disorder, the condition $\rho = 0$ can be satisfied for all layers simultaneously, when ε and/or μ fluctuate, the conditions (27) or (28) define the frequency-dependent Brewster angles which are slightly different for different layers. These angles occupy an interval within which *both homogeneous or mixed stacks* are not completely transparent, but have anomalously large transmission lengths.[28,31]

When only the dielectric permittivity is disordered and $\mu = \overline{\mu}$, the Brewster conditions (27), (28) simplify to

$$\tan^2 \theta_s = -1, \tag{29}$$

$$\tan^2 \theta_p = \frac{\varepsilon}{\overline{\varepsilon}} \approx 1. \tag{30}$$

Hence, in the presence of only permittivity disorder, the Brewster condition is satisfied only for *p* polarization. Since the disorder is weak, i.e., $\varepsilon \approx \overline{\varepsilon}$, the Brewster angle of incidence

from the effective medium is $\theta_p \approx \pi/4$. The corresponding angle from free space, θ_a, is related to the Brewster angle θ_p through Snell's law, and for the given θ_a, the Brewster frequency f_p follows from

$$\sqrt{\varepsilon(f_p)\overline{\mu}(f_p)} = \frac{\sin \theta_a}{\sin \theta_p} = \sqrt{2}\sin \theta_a. \tag{31}$$

Note that this equation may be satisfied at multiple frequencies depending on the form of the dispersion.

In the case of only magnetic permeability disorder, $\varepsilon = \overline{\varepsilon}$, the Brewster conditions (27), (28) reduce to [compare with Eqs. (29) and (30)]

$$\tan^2 \theta_s = \frac{\mu}{\overline{\mu}} \approx 1, \tag{32}$$

$$\tan^2 \theta_p = -1, \tag{33}$$

and the Brewster anomaly is observed for *s* polarization at the Brewster frequency f_s given by

$$\sqrt{\varepsilon(f_s)\mu(f_s)} = \frac{\sin \theta_a}{\sin \theta_s} = \sqrt{2}\sin \theta. \tag{34}$$

For disorder in both the permeability and the permittivity, the existence of a Brewster anomaly angle depends, in accordance with Eqs. (27) and (28), on the sign of the quantity $\xi = (\overline{\varepsilon}\mu - \varepsilon\overline{\mu})/(\varepsilon\mu - \overline{\varepsilon}\,\overline{\mu})$. If $\xi > 0$, the Brewster angle exists for *s* polarization, while if $\xi < 0$, it exists for *p* polarization. In the case $\xi = 0$, the layer and the medium in which it is embedded are impedance matched, and thus the layer is completely transparent.

III. NUMERICAL RESULTS

A. Metamaterial stack

Along with the analytical calculations a comprehensive numerical study of the properties of the transmission length as a function of wavelength and angle of incidence has been carried out. We first consider the case of normal incidence on a stack of $N = 10^7$ layers, in which we randomize only the dielectric permittivity ($Q_m = 0$) with $Q_e = 0.5 \times 10^{-2}$. Figure 2 displays the transmission length l_T as a function of frequency f. The upper curves present the case in which absorption is neglected, while the lower curves show the effects of absorption. The red solid curves and the blue dashed curves display results from numerical simulations and the theoretical prediction (18), respectively. The top curves represent the genuine localization length for all frequencies except those in the vicinity of $f \approx f_{mp} = 10.95$ GHz where the transmission length dramatically increases.

In the absence of absorption, for frequencies $f > 10.95$ GHz, the metamaterial transforms from being double negative to single negative (see inset in Fig. 2). The refractive index of the metamaterial layer changes from being real to being purely imaginary, the random stack becomes opaque, and the transmission length substantially decreases. Such a drastic change in the transmission length (by a factor of 10^5) might be able to be exploited in a frequency-controlled optical switch.

The theoretical result (18) is in excellent agreement with simulation based on the exact recurrence relations (7) and (8) across the frequency interval 10.4 GHz $< f <$ 11.0 GHz.
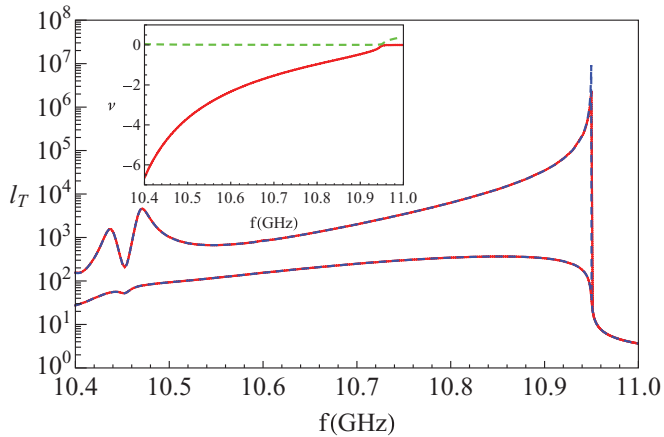
FIG. 2. (Color online) Transmission length l_T vs frequency f at normal incidence ($\theta_a = 0$) for a metamaterial stack without absorption (top curve) and in the presence of the absorption (bottom curves). Red solid curves display numerical simulations while blue dashed curves show the analytical predictions. Inset: The real (red solid line) and imaginary (green dashed line) part of the metamaterial layer refractive index.
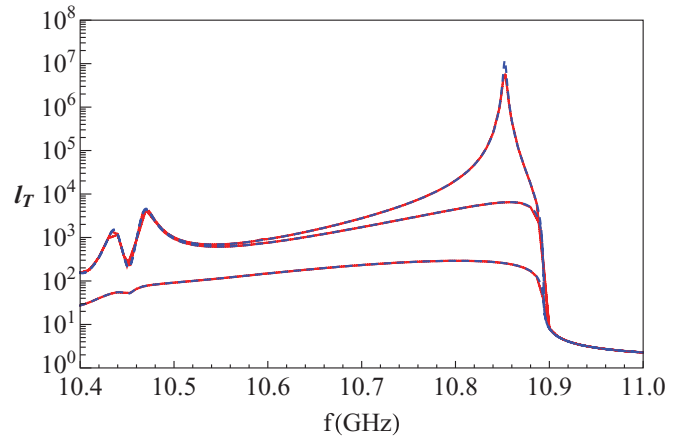

FIG. 3. (Color online) Transmission length l_T vs frequency f for $\theta_a = 30°$ for a metamaterial stack: without absorption, p polarization (top curves), s polarization (middle curves); in the presence of absorption (bottom curves). Results for numerical simulations (red solid curves) and analytical predictions Eq. (18) (blue dashed curves) are shown.

Moreover, the first term in Eq. (18), corresponding to the single-scattering approximation, dominates for all frequencies except in the region 10.4 GHz $< f <$ 10.5 GHz where both terms in Eq. (18) are necessary to describe the localization length. Quite surprisingly, the asymptotic equations (20) and (26) are in excellent agreement with the numerical results over the frequency range 10.9 GHz $< f <$ 11.0 GHz, including in the near vicinity of the frequency $f_{mp} = 10.95$ GHz at which μ vanishes.

Absorption substantially influences the transmission length (the lower curve in Fig. 2) and smooths the nonmonotonic behavior of the transmission length for $f <$ 10.5 GHz. The small dip at $f \approx 10.45$ GHz correlates with the corresponding dip in the transmission length in the absence of absorption. The most prominent effect of absorption occurs for frequencies just below the μ-zero frequency $f_{mp} = 10.95$ GHz. While in the absence of absorption, the stack is nearly transparent in this region, turning on the absorption reduces the transmission length by a factor of 10^2–10^3 for $f >$ 10.7 GHz. In contrast, for frequencies $f >$ 10.95 GHz, the transmission lengths in the presence and absence of absorption are nearly identical because here the stack is already opaque and its transmittance is not much affected by an additional small amount of absorption. Again, the simulations and the theoretical predictions are in excellent agreement and show that the theoretical form (18) accounts accurately for dissipation.

The transmission length spectrum in the case where both disorders of the dielectric permittivity and magnetic permeability are present, i.e., $Q_e = Q_m = 0.5 \times 10^{-2}$, is qualitatively similar to that of the single-disorder case considered above, and so we do not present these results here.

In the case of *oblique incidence*, polarization effects become important. In Fig. 3, we display the transmission length frequency spectrum for a homogeneous metamaterial stack with only dielectric permittivity disorder for the angle of incidence $\theta_a = 30°$. For frequencies $f <$ 10.55 GHz, the transmission length is largely independent of the polarization.

Moreover it does not differ from that for normal incidence (compare with the top curve in Fig. 2). This is due to the high values of the refractive indices at these frequencies ($|\nu_n| > 4$), resulting in almost zero refraction angles (14) for angles of incidence that are not too large.

As noted previously, true delocalization, such as in the presence of only thickness disorder, cannot occur for material disorder (i.e., permittivity or permeability disorder). Nevertheless, the transmission length manifests a sharp maximum at an angle close to the Brewster angle, as commented upon in Refs. 28 and 31. This is indeed apparent in Fig. 3 for the frequency $f \approx 10.85$ GHz. Because only ε fluctuates, the Brewster condition is satisfied only for p polarization (30) at a single frequency $f_p \approx 10.852$ GHz. The introduction of additional permeability disorder (not shown) reduces the maximum value of the localization length by two orders of magnitude.

Comparison of Figs. 2 and 3 shows that the frequency of the maximal suppression of localization decreases as the angle of incidence increases. At normal incidence it coincides with the μ-zero frequency f_{mp} while for oblique incidence at $\theta_a = 30°$ it coincides with the Brewster frequency f_p for p polarization.

Absorption strongly diminishes the transmission length. In Fig. 3, we display results of numerical simulations of the transmission length for p polarization (bottom red solid curve) and the corresponding theoretical prediction (18) (blue dashed curve). Both curves are almost identical, with absorption providing the main contribution to the transmission length, and with the permittivity disorder having little influence on the transmission length. The results for s polarization are therefore practically indistinguishable from those for p polarization.

The transmission properties of a stack *with only magnetic permeability disorder at oblique incidence* are similar to those for the case of only dielectric permittivity disorder. In Fig. 4 we plot the transmission length as a function of frequency at the incidence angle $\theta_a = 30°$. The key difference is that there is a Brewster anomaly for s polarization (top curves in Fig. 4) while for p polarization (middle curves in Fig. 4) the Brewster
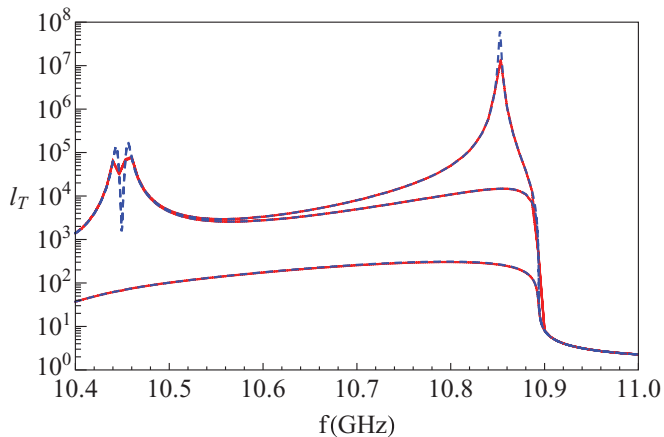
FIG. 4. (Color online) Transmission length l_T vs frequency f at $\theta_a = 30°$ for a metamaterial stack with the magnetic permeability disorder: without absorbtion, s polarization (top curve), p polarization (middle curve); in the presence of the absorbtion (bottom curves). Red solid curves are simulation results while the blue dashed curves are analytical predictions, Eq. (18).
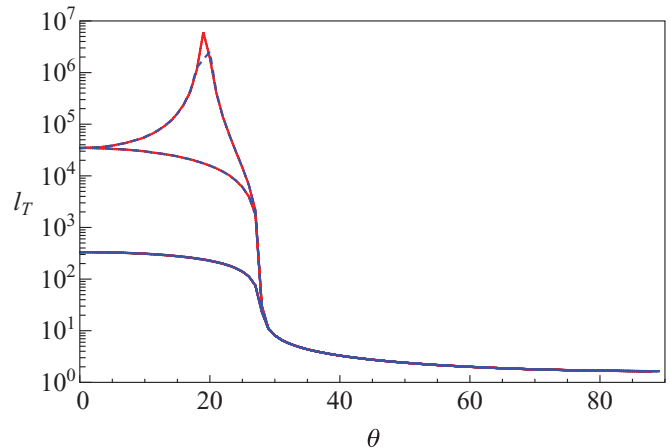

FIG. 5. (Color online) Transmission length l_T vs angle of incidence for a homogenous metamaterial stack at $f = 10.7$ GHz with permittivity disorder: in the absence of absorption—upper curve and for p polarization; middle curve is for s polarization and in the presence of absorption; and for both polarizations, lower curves. The solid red lines are the numerical simulations and the blue dashed lines are the theoretical predictions, Eq. (18).

anomaly is absent. The effect of absorption (the bottom curves) is also similar to that of the preceding case.

We finally consider the dependence of the transmission length on the angle of incidence at a fixed frequency. The results for both polarizations are displayed in Fig. 5. Here we have plotted the transmission length of the stack *with only dielectric permittivity disorder* with $Q_e = 0.5 \times 10^{-2}$ at the frequency $f = 10.90$ GHz, as a function of the angle of incidence. The upper and middle curves correspond to the results for p- and s-polarized waves, respectively, in the absence of absorption. For s-polarized light, the transmission length decreases monotonically with increasing angle of incidence, while for p-polarized waves it increases with increasing angle of incidence. Such behavior reflects the existence of a Brewster angle for p polarization at the Brewster angle $\theta_a = 15°$. The red solid curve shows the results of simulations, while the blue dashed line is the analytic prediction based on Eq. (18).

As in the previous cases, in the presence of absorption, the results for both polarizations are almost identical (the lower curves in Fig. 5). For angles $\theta_a < 30°$, the transmission length is dominated by absorption, while for angles $\theta_a > 30°$ tunneling is the dominant mechanism. The results for permeability disorder (not presented) are very similar to those for permittivity disorder.

B. Normal-material stacks

1. Standard normal stacks

According to the definitions of Sec. II A, in a homogeneous normal layer the dielectric permittivity and the magnetic permeability are defined as $-\varepsilon^*(f)$ and $-\mu^*(f)$, respectively, with $\varepsilon(f)$ and $\mu(f)$ given by Eqs. (1) and (2). For such a layer the refractive index is positive in the region 10.40 GHz $< f < 10.95$ GHz. At higher frequencies 10.95 GHz $< f < 11.00$ GHz, the magnetic permittivity becomes negative and we now deal with a SNM. The transmission length in this case manifests exactly the same behavior as for stacks comprised

of metamaterial layers that were considered in the previous Sec. III A.

2. Exotic normal stacks

The most unusual features of the transmission length appear in the vicinities of the μ-zero and/or ε-zero frequencies and at the Brewster frequency. In this section, we consider a model, which although being rather artificial, offers extraordinary transport properties that could be useful for designing optical switching devices. Within this model, the dielectric permittivity coincides with that of the normal material, $-\varepsilon^*(f)$, over the entire frequency range 10.40 GHz $< f < 11.00$ GHz,, while the magnetic permeability coincides with that of normal material, $-\mu^*(f)$, only in the region 10.40 GHz $< f < 10.95$ GHz, with its values at higher frequencies, 10.95 GHz $< f < 11.00$ GHz, being given by Eq. (2) (metamaterial). It is easy to see that the refractive index is always positive and is practically symmetric $[\mu(f) \propto |f - f_{mp}|]$ about the frequency $f_{mp} = 10.95$ GHz, at which it vanishes. As a consequence, when this frequency is crossed, the transmission length of a random stack of such layers manifests an abrupt switching from complete transparency (at normal incidence) to strong localization (i.e., strong reflection) at oblique incidence. Therefore, the transmission length, in the case of normal incidence, must manifest the same symmetry in the vicinity of this frequency. Note that qualitatively the transmission behavior would have been the same as observed here if the frequency model for μ behaved according to the form $\mu(f) \propto (f - f_{mp})^2$ rather than $\mu(f) \propto |f - f_{mp}|$. Note that the former does not violate the Kramers-Kronig condition and as a consequence the transmission characteristics depicted below are possible.

The normal incidence transmission length, as a function of wavelength, is plotted in Fig. 6 for stacks of $N = 10^7$ layers with only dielectric permittivity disorder $Q_e = 0.5 \times 10^{-2}$, $Q_m = 0$. The upper and lower curves display $l_T(f)$ for lossless
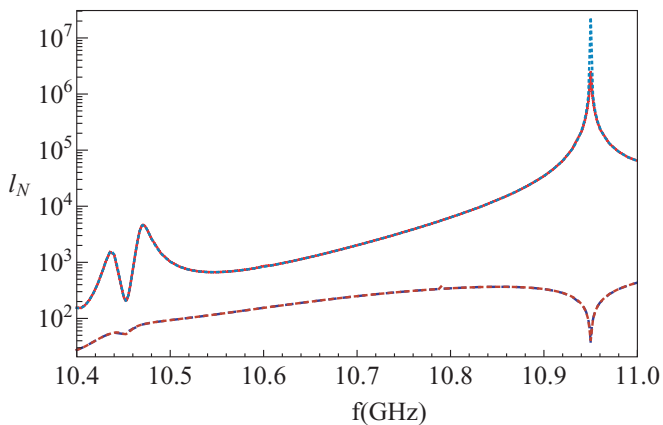
FIG. 6. (Color online) Transmission length l_T vs frequency f at normal incidence for a homogeneous stack: without absorption (upper curve), and in the presence of absorbtion (lower curves). The red solid curves are the numerical simulations and the blue dotted lines are Eq. (18).

and absorbing stacks, respectively. The red solid curves and the dashed blue curves display, respectively, the results of numerical simulations and the theoretical prediction (18). The upper curves, corresponding to an absence of absorption, represent the genuine localization length for all frequencies except for the vicinity of $f \approx f_{mp} = 10.95$ GHz, where the transmission length drastically increases. For frequencies $f < f_{mp} = 10.95$ GHz, the transmission length coincides with that of the normal or metamaterial stack (see Fig. 2), while for frequencies f slightly exceeding the characteristic frequency f_{mp} the symmetry mentioned above is clearly manifest. Absorption (lower curve in Fig. 6) has a similar effect on the transmission length as that shown for metamaterial stacks.

We have plotted (see Fig. 7 top curve) the same curve for an angle of incidence $\theta_a = 5°$. The corresponding curve demonstrate a deep dip (four orders of magnitude) in the transmission length over the narrow frequency range 10.93 GHz $< f <$
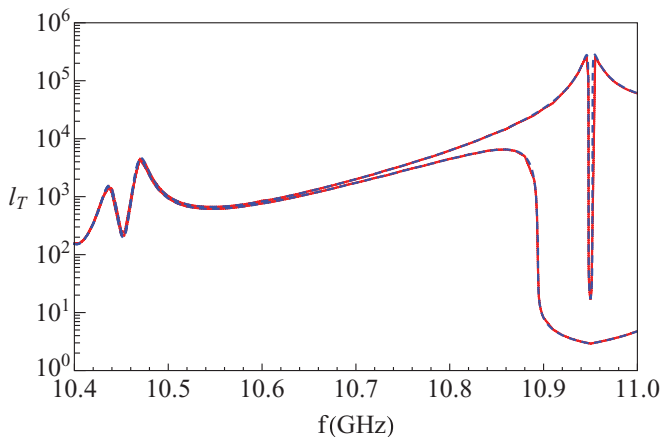

FIG. 7. (Color online) Transmission length l_T vs frequency f for *s*-polarized, off-axis incidence $\theta_a = 5°$ top curve and for $\theta_a = 30°$ bottom curve for a normal material stack in the absence of absorbtion. The red solid curves are numerics and the blue dashed curves are the theoretical predictions, Eq. (18).

10.97 GHz. The origin of the dip is related to the tunneling nature of wave propagation at these frequencies.

The width of the strong localization region (where the transmission length becomes comparatively small) increases with increasing angle of incidence. For $\theta_a = 30°$ and s polarization, this range is 10.85 GHz $< f < 11$ GHz (lower, dashed, blue line in Fig. 7) and corresponds to the tunneling regime. For frequencies $f < 10.85$ GHz, the localization length coincides with the localization length for a metamaterial stack (see middle curve in Fig. 2).

The results for p polarization are similar to those for s polarization (with the exception that the transmission length has its maximum at $\theta = 30°$ at $f \approx 10.85$ GHz), and thus we do not present them here.

C. Mixed stacks

The case of mixed stacks without thickness disorder is very interesting. It is shown in Ref. 10 that, for a nondispersive mixed stack with fluctuating refractive indices and constant layer widths, localization of long-wavelength radiation is strongly suppressed. This suppression manifests itself as the anomalous, $l \propto \lambda^6$, growth of the localization length in the long-wave region instead of the usual dependence $l \propto \lambda^2$. To study how dispersion influences this effect we consider transmission through mixed stacks with only dielectric permittivity disorder.

In Fig. 8(a), we plot the transmission length spectrum in the case of normal incidence, for a small permittivity disorder of $Q_e = 0.5 \times 10^{-2}$, and observe significant (up to four orders of magnitude) suppression of localization in the frequency region 10.50 GHz $< f < 10.68$ GHz. However, in this case the localization length grows with increasing frequency, while, in Ref. 10, similar growth has been observed with increasing incident wavelength. This is shown in Fig. 8(b) where the same transmission length spectrum is plotted as a function of free-space wavelength. Thus, the localization length decreases by four orders of magnitude, manifesting as an enhancement, rather than the suppression, of localization with increasing wavelength.

Although at first sight these findings are in sharp contrast, both are correct and physically meaningful. In the model studied in Ref. 10, the wavelength of the incident radiation largely coincided with the wavelength inside each layer. In the problem that we consider here, these two wavelengths differ substantially. Accordingly, in Fig. 8(c), we plot the transmission length as a function of wavelength within the stack and obtain results which are very similar to those in Ref. 10. To emphasize the similarity with Fig. 3 in Ref. 10, we have plotted the transmission length spectrum for three different stack lengths: $N = 10^5, 10^6, 10^7$. It is easily seen that the suppression of localization in the dispersive media is qualitatively and quantitatively similar to that predicted in Ref. 10. Indeed, the suppression observed there was described by a power law $l_T \propto \lambda^6$, with subsequent more detailed calculations[15] correcting the estimate of this power from 6 to 8.78. The results in Fig. 8(c) correspond to a power of 8.2. The lower curves in Figs. 8(a)–8(c) correspond to samples with both types of disorder $Q_e = Q_m = 0.5 \times 10^{-2}$ and are very well described by the analytical prediction (19) with $l \propto \lambda^2$.
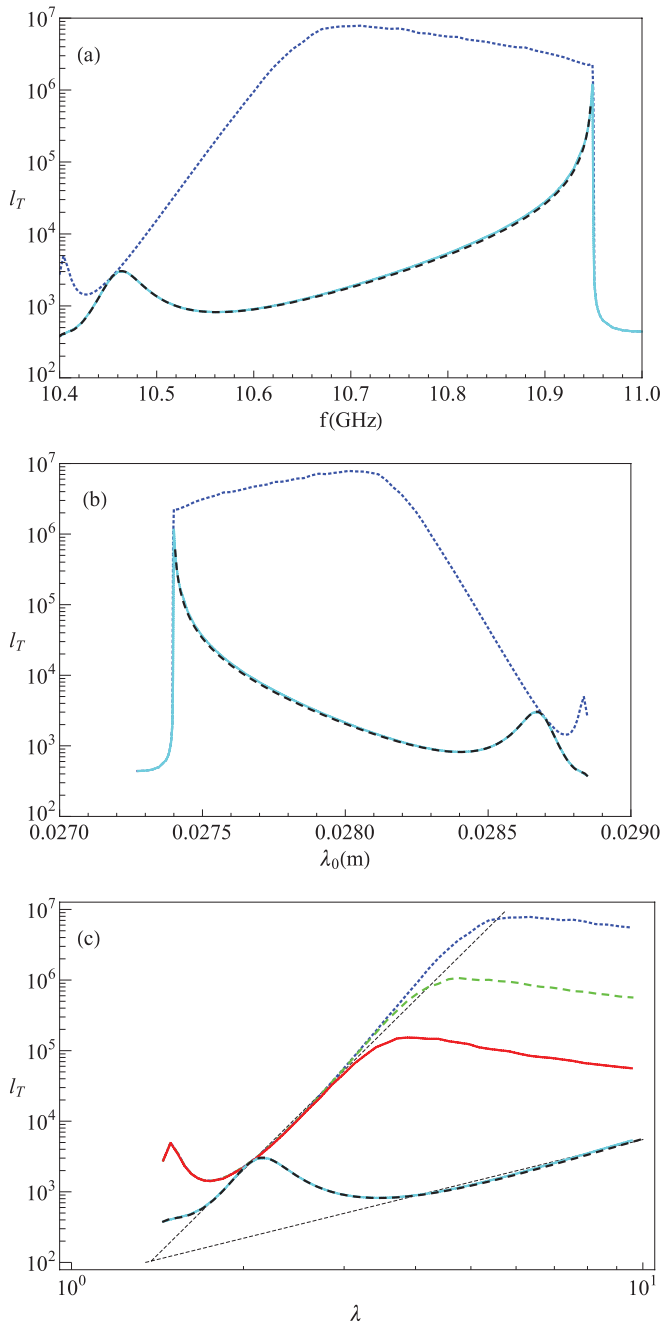
FIG. 8. (Color online) (a) Transmission length l_T vs frequency f for a mixed stack with $N = 10^7$ layers (top dotted blue curve), and only dielectric permittivity disorder. The bottom curves on all three panels are for a stack with $N = 10^7$ layers with both permittivity and permeability disorder (the cyan solid curve displays simulation results while the dashed black curve is for the analytic prediction, Eq. (19); (b) is the same as in (a) but plotted as a function of the free-space wavelength λ_0 while on panel (c) we plot the transmission length as a function of the averaged wavelength inside the stack normalized to the thickness of the layer, for $N = 10^7$ layers (blue dotted top curve), $N = 10^6$ layers (dashed green curve), and for $N = 10^5$ layers (red solid curve).

Combining the results of this section with those obtained previously,[10,15] we may conclude that dielectric permittivity disorder in mixed stacks having constant layer thickness is not sufficiently strong to localize low-frequency radiation. To obtain the "typical" long-wavelength behavior of the localization length, $\propto \lambda^2$, one has to "switch on" additional disorder—either thickness disorder as in Refs. 10 and 15 or magnetic permeability disorder as in the present work.

The transmission length obtained here remains very large up to the μ-zero frequency $f_{mp} = 10.95$ GHz [Fig. 8(a)]. This leads us to hypothesize that suppression of localization in the model considered here is related to the vanishing of the effective magnetic permeability at $f = f_{mp}$. In this case, one should expect a substantial increase of the localization length with increasing frequency and a sharp peak of the localization length at $f = f_{mp}$. However, the stack of $N = 10^7$ layers is too short for this to occur, and thus its localization regime is bounded from above by the frequency $f = 10.65$ GHz. Therefore, we do not observe the expected peak at $f = 10.95$ GHz. However, we do observe the abrupt drop of the localization length as we approach this frequency from the right. Thus, we conclude that we are dealing with the same effect of delocalization at μ-zero frequency as was observed in monotype samples (see Fig. 2). However, in contrast to the latter case, the corresponding growth of the localization length begins essentially earlier and occurs substantially faster.

IV. CONCLUSION

Transport and localization of classical waves in one-dimensional disordered systems containing dispersive, lossy metamaterials have been studied analytically and numerically. It has been shown that the field can be delocalized in one-dimensional μ-near-zero or ε-near-zero media—a new form of delocalization that occurs in one dimension in the presence of short-correlated disorder. We have also demonstrated disspersion-induced suppression of Anderson localization in mixed stacks with either dielectric permittivity or magnetic permeability disorder. The presence of both forms of disorder, however, enhances localization. The effects of polarization in the presence of different forms of disorder have been studied and Brewster anomalies have been demonstrated at angles (or frequencies) that depend not only on the polarization of the radiation, but also on the type of disorder. The theoretical predictions are in excellent agreement with the results of numerical simulations.

APEENDIX: DERIVATION OF EQ. (6)

Here we provide an outline of the derivation of Eq. (6) and assume that the disordered stack with N layers is embedded in a homogeneous infinitesimal medium with material parameters given by $\bar{\varepsilon} = \langle \varepsilon \rangle$ and $\bar{\mu} = \langle \mu \rangle$, where ε and μ are given by Eqs. (1) and (2), respectively. The impedance and refractive index of the medium are $Z_b = \sqrt{\bar{\mu}/\bar{\varepsilon}}$ and $v_b = \sqrt{\bar{\mu}}\sqrt{\bar{\varepsilon}}$, respectively.
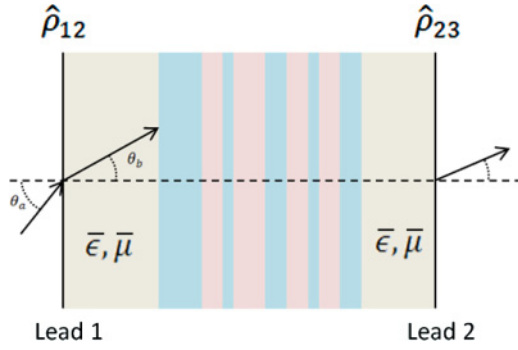
FIG. 9. (Color online) The disordered stack is embedded in a homogeneous medium with averaged material parameters $\overline{\varepsilon}$, $\overline{\mu}$.

This random stack is sandwiched between two leads connecting the outside free space and the homogeneous medium ($\overline{\varepsilon}$, $\overline{\mu}$) (see Fig. 9). The right lead reflection coefficient for left-hand incidence is

$$\hat{\rho}_{23} = \frac{\mathcal{Z}_b \cos \theta_b - \mathcal{Z}_a \cos \theta_a}{\mathcal{Z}_b \cos \theta_b + \mathcal{Z}_a \cos \theta_a}, \quad \text{(A1)}$$

and

$$\cos \theta_b = \sqrt{1 - \frac{\sin^2 \theta_a}{v_b^2}}, \quad \text{(A2)}$$

while the transmission coefficient is given by $\hat{\tau}_{23} = 1 + \hat{\rho}_{23}$. The front (left) "lead" reflection and transmission coefficients for incidence from the left side are given by $\hat{\rho}_{12} = -\hat{\rho}_{23}$ and $\hat{\tau}_{12} = 1 + \hat{\rho}_{12}$, respectively.

The total transmission coefficient $T_N(\theta_a)$ through such a structure with both Fresnel "leads" in place can be calculated from

$$T_N(\theta_a) = \frac{\hat{\tau}_{23} \hat{T}_N(\theta_b) \hat{\tau}_{12}}{(1 - \hat{R}_N \hat{\rho}_{21})(1 - \hat{R}'_N \hat{\rho}_{23}) - \hat{\rho}_{21} \hat{T}_N \hat{\rho}_{23} \hat{T}'_N}, \quad \text{(A3)}$$

where $\hat{T}_N(\theta_b)$ is the transmission of a random stack with N layers embedded in homogeneous medium with $\overline{\varepsilon}$ and $\overline{\mu}$, for plane-wave incidence from the left with incident angle θ_b, and with $\hat{\rho}_{21} = \hat{\rho}_{23}$. The terms $\hat{R}_N$ and $\hat{R}'_N$ are reflection coefficients for the random stack for plane-wave incidence from the left/right sides, while the $\hat{T}'_N$ is the transmission coefficient for incidence from the right.

In the localized regime as $N \to \infty$, the transmission coefficient $T_N(\theta_a) = \hat{T}'_N(\theta_b) \to 0$ and therefore the final term in the denominator of Eq. (A3) vanishes. Accordingly,

$$\ln T_N(\theta_a) = \ln \hat{T}_N(\theta_b) + \ln \hat{\tau}_{23} + \ln \hat{\tau}_{12}$$
$$- \ln(1 - \hat{R}_N \hat{\rho}_{21}) - \ln(1 - \hat{R}'_N \hat{\rho}_{23}). \quad \text{(A4)}$$

As $N \to \infty$, the last four terms in Eq. (A4) are bounded and we deduce

$$\lim_{N \to \infty} \frac{\ln T_N(\theta_a)}{N} = \lim_{N \to \infty} \frac{\ln \hat{T}_N(\theta_b)}{N}. \quad \text{(A5)}$$

Thus, the localization length for a stack embedded in free space for plane-wave incidence at an angle θ_a is equivalent to calculating the localization length for a stack of N layers embedded in a medium with the refractive index v_b with plane-wave incidence at an angle θ_b. The angles θ_a and θ_b are related by Snell's law [Eq. (14)]. From Eq. (A5), we thus deduce the relation in Eq. (6).

[1]P. W. Anderson, Phys. Rev. **109**, 1492 (1958).

[2]E. Abrahams (ed.), *50 Years of Anderson Localization* (World Scientific, Singapore, 2010).

[3]P. Marcos and C. M. Soukoulis, *Wave Propagation from Electrons to Photonic Crystals and Left-Handed Materials* (Princeton University Press, Princeton, 2008).

[4]V. G. Veselago, Sov. Phys. Usp. **10**, 509 (1968).

[5]J. B. Pendry, Phys. Rev. Lett. **85**, 3966 (2000).

[6]K. Yu. Bliokh and Yu. P. Bliokh, Phys. Usp. **47**, 393 (2004); Usp. Fiz. Nauk **174**, 439 (2004).

[7]T. Terao, Phys. Rev. E **82**, 026702 (2010).

[8]M. V. Gorkunov, S. A. Gredeskul, I. V. Shadrivov, and Yu. S. Kivshar, Phys. Rev. E **73**, 056605 (2006).

[9]Y. Dong and Z. Zhang, Phys. Lett. A **359**, 542 (2006).

[10]A. A. Asatryan, L. C. Botten, M. A. Byrne, V. D. Freilikher, S. A. Gredeskul, I. V. Shadrivov, R. C. McPhedran, and Yu. S. Kivshar, Phys. Rev. Lett. **99**, 193902 (2007).

[11]F. M. Izrailev and N. M. Makarov, Phys. Rev. Lett. **102**, 203901 (2009).

[12]D. Mogilevtsev, F. A. Pinheiro, R. R. dos Santos, S. B. Cavalcanti, and L. E. Oliveira, Phys. Rev. B **82**, 081105(R) (2010).

[13]E. Reyes-Gómez, A. Bruno-Alfonso, S. B. Cavalcanti, and L. E. Oliveira, Phys. Rev. E **84**, 036604 (2011).

[14]D. Mogilevtsev, F. A. Pinheiro, R. R. dos Santos, S. B. Cavalcanti, and L. E. Oliveira, Phys. Rev. B **84**, 094204 (2011).

[15]A. A. Asatryan, S. A. Gredeskul, L. C. Botten, M. A. Byrne, V. D. Freilikher, I. V. Shadrivov, R. C. McPhedran, and Yu. S. Kivshar, Phys. Rev. B **81**, 075124 (2010).

[16]F. M. Israilev, N. M. Makarov, and E. J. Torres-Herrera, Physica B **405**, 3022 (2010).

[17]E. J. Torres-Herrera, F. M. Israilev, and N. M. Makarov, Low Temp. Phys. **37**, 1201 (2011).

[18]E. J. Torres-Herrera, F. M. Israilev, and N. M. Makarov, e-print arXiv:1111.3397.

[19]P. Han, C. T. Chan, and Z. Q. Zhang, Phys. Rev. B **77**, 115332 (2008).

[20]A. A. Asatryan, N. A. Nicorovici, L. C. Botten, C. M. de Sterke, P. A. Robinson, and R. C. McPhedran, Phys. Rev. B **57**, 13535 (1998).

[21]M. G. Silveirinha and N. Engheta, Phys. Rev. Lett. **97**, 157403 (2006).

[22]A. Alu, M. G. Silveirinha, A. Salandrino, and N. Engheta, Phys. Rev. B **75**, 155410 (2007).

[23] E. Liznev, A. Dorofeenko, L. Huizhe, A. Vinogradov, and S. Zouhdi, Appl. Phys. A **100**, 321 (2010).

[24] L. Liu, C. Hu, Z. Zhao, and X. Luo, Opt. Express **17**, 12183 (2009).

[25] B. Edwards, A. Alu, M. E. Young, M. Silveirinha, and N. Engheta, Phys. Rev. Lett. **100**, 033903 (2008).

[26] R. A. Shelby, D. R. Smith, and S. Schultz, Science **292**, 77 (2001).

[27] D. R. Smith, Phys. Rev. E **81**, 036605 (2010).

[28] A. A. Asatryan, L. C. Botten, M. A. Byrne, V. D. Freilikher, S. A. Gredeskul, I. V. Shadrivov, R. C. McPhedran, and Y. S. Kivshar, Phys. Rev. B **82**, 205124 (2010).

[29] P. W. Milonni, *Fast Light, Slow Light, and Left-Handed Light* (Dirac House, Bristol, 2005).

[30] X. Huang, Y. Lai, Z. H. Hang, H. Zeng, and C. T. Chan, Nature Mater. **10**, 582 (2011).

[31] J. E. Sipe, P. Sheng, B. S. White, and M. H. Cohen, Phys. Rev. Lett. **60**, 108 (1988).